Received: 2 February 2018 | Revised: 8 April 2018 | Accepted: 11 April 2018
DOI: 10.1002/ardp.201800023

FULL PAPER

DPhG ARCH PHARM
Archiv der Pharmazie

Anticancer activity of dihydropyrazolo[1,5-*c*]quinazolines against rat C6 glioma cells via inhibition of topoisomerase II

Gagandeep Kaur[1] | Ravi P. Cholia[2] | Gaurav Joshi[1] | Suyog M. Amrutkar[3] | Sourav Kalra[4] | Anil K. Mantha[2] | Uttam C. Banerjee[3] | Raj Kumar[1]

[1] Laboratory for Drug Design and Synthesis, Department of Pharmaceutical Sciences and Natural Products, Central University of Punjab, Bathinda, India

[2] Department of Animal Sciences, Central University of Punjab, Bathinda, India

[3] Department of Pharmaceutical Technology (Biotechnology), National Institute of Pharmaceutical Education and Research (NIPER), S. A. S. Nagar, Mohali, India

[4] Department of Human Genetics and Molecular Medicine, Central University of Punjab, Bathinda, India

Correspondence
Dr. Raj Kumar, Laboratory for Drug Design and Synthesis, Department of Pharmaceutical Sciences and Natural Products, Central University of Punjab, 151 001 Bathinda, India.
Email: raj.khunger@gmail.com, rajcps@cup.ac.in

Funding information
Bristol-Myer Squibb, USA, Grant number: 34003085

Abstract

The design and synthesis of dihydropyrazolo[1,5-*c*]quinazolines (**1a–h**) as human topoisomerase II (TopoII) catalytic inhibitors are reported. The compounds were investigated for their antiproliferative activity against the C6 rat glial cell line. Two compounds, **1b** and **1h**, were found to be potent cytotoxic agents against glioma cells and exerted selective TopoII inhibitory activity. Furthermore, the compounds induced alterations in reactive oxygen species levels as measured by DCFDA assay and were found to induce cell cycle arrest at the G1 phase at lower concentrations and profound apoptosis at higher concentrations. The interaction of selected investigational molecules with TopoII was further corroborated by molecular modeling.

KEYWORDS
cancer, cell cycle, dihydropyrazolo[1,5-*c*]quinazoline, rat C6 glioma cells, topoisomerases

1 | INTRODUCTION

Topoisomerases (Topo) are designated as the magicians in the world of DNA.[1,2] They are associated with resolving all the topological problems of DNA. Their overexpression is found in various diseases including cancer.[3] Human DNA topoisomerases are classified into topoisomerase I (TopoI) and topoisomerase II (TopoII) and are considered to be the authenticated targets for numerous classes of potent anti-cancer drugs including epipodophyllotoxin, etoposide, and the anthracycline derivative doxorubicin, camptothecin, etc.[2,4,5] The TopoI is involved in breakage of the DNA single strand whereas TopoII is known to cleave double strand of phosphate backbone of the DNA and needs ATP for its function irrespective of hTopoI.[6] The clinically active hTopoII inhibitors induce cancer cell death by trapping TopoII-DNA complex (covalent complex), subsequently leading to DNA damage.[7] Numerous studies in the past have correlated the overexpression of hTopoII as a prognostic marker in the glioblastomas (GBMs).[8] GBM is considered as the severe and the most aggressive form of malignant brain tumor.[9] The TopoII is a well-validated target for GBM chemotherapy.[10,11] Several topoisomerase inhibitors (poison and catalytic) from natural and synthetic origin act at different phases of the catalytic cycle.[12–15] Additionally, TopoII inhibitors are reported to exhibit lack of isoform specificity and multidrug resistance in tumor cells. Submicromolar inhibitory values of available TopoII inhibitory drugs have rendered many opportunities to explore this research area.[16,17] Through our previous experiences in the field of anticancer drug discovery and development,[18–24] we thought of designing dihydropyrazolo[1,5-*c*]quinazolines (**1**) as TopoII catalytic inhibitors after considering the interaction models of phosphoraminophosphonic acid–adenylate ester (ANP), an ATP analog, as well as *N*-acetyl pyrazoline (**2**),[19] previously reported TopoII inhibitor

Gagandeep Kaur and Ravi P. Cholia have contributed equally to this paper.

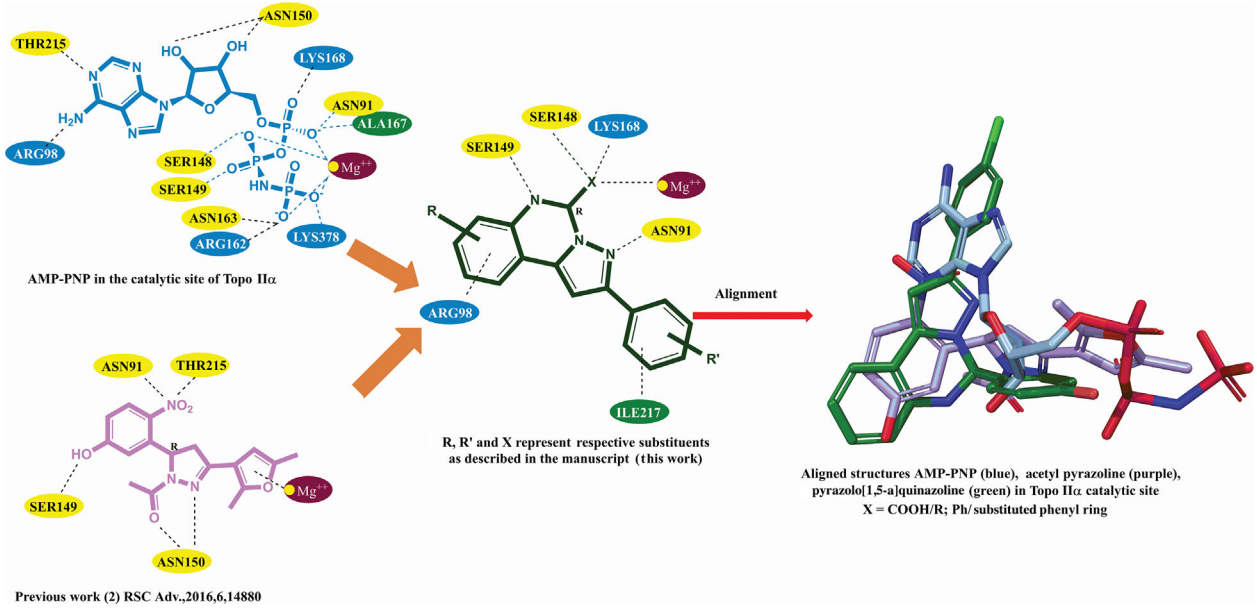

FIGURE 1 Design of target compounds (**1**) as topoisomerase II inhibitors

(Figure 1) at the catalytic domain of hTopoII enzyme (PDB entry: 1ZXM).[25] The rationale behind the design of **1** includes that (a) two aryl groups be flanked by a central heteroaromatic ring and one of the rings should be able to coordinate with Mg^{2+} center of TopoII; (b) *N*-$COCH_3$ of **2** may be isosterically replaced with cyclized N-C-N-Ar rigid framework in order to increase stability and avoid acid mediated cleavage that can occur with acetamido group of **2** in tumor microenvironment; and (c) extra phenyl ring may not only impart necessary lipophilicity to **1** to cross the blood brain barrier in GBM but may also get into the hydrophobic cavity of ATP domain in hTopoII. With this background, we herein report the synthesis and biological evaluation of **1** (Figure 1).

2 | RESULTS AND DISCUSSION

2.1 | Chemistry

Compounds **6a**,**b** as precursors for the synthesis of the target compounds **1a**–**h** were prepared by using synthetic procedures shown in Scheme 1. Briefly a mixture of 2-nitrobenzaldehyde (**A**) and appropriate aryl ketone (**B**) in glacial acetic acid was stirred using conc. H_2SO_4 as catalyst to afford appropriate 1,3-diaryl propenone (**3a**, **b**)[19,26,27] which on reaction with hydrazine hydrate in methanol yielded appropriate pyrazoline (**4a**,**b**).[19,26,27] The pyrazolines so obtained were further oxidized in the presence of I_2/DMSO to yield pyrazole derivatives (**5a**,**b**). The aromatic nitro group of the appropriate pyrazoles was reduced using $SnCl_2$-HCl in methanol to procure the intermediates aryl-*1H*-pyrazol-5-yl anilines (**6a**,**b**).

2.1.1 | Synthesis of dihydropyrazolo[1,5-*c*]quinazoline derivatives as target molecules (1a–h)

The intermediates aryl-*1H*-pyrazol-5-yl anilines (**6a**,**b**) so formed were cyclo-condensed with glyoxylic acid as well as with aryl aldehydes to afford the target dihydropyrazolo[1,5-*c*]quinazoline compounds (**1a–h**; Figure 2). All the final compounds were characterized by ^1H, ^{13}C NMR, IR, mass, and elemental analyses.

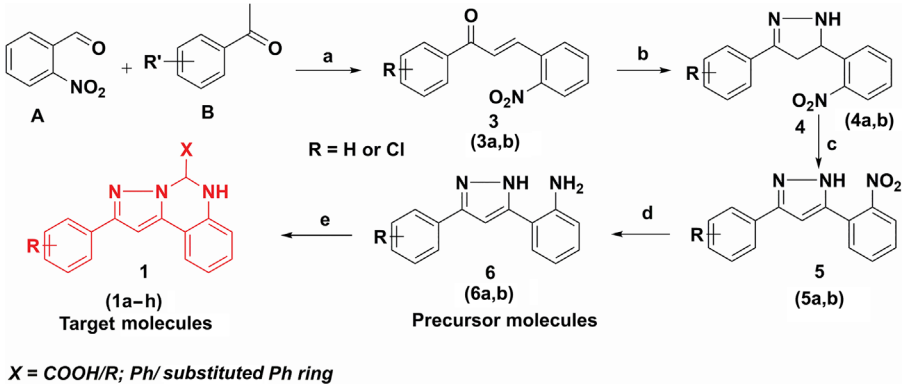

SCHEME 1 Synthesis of the target molecules **1a–h**. Reagents and conditions (a) CH_3COOH, H_2SO_4 (1 drop), rt, 24 h; (b) $NH_2NH.H_2O$, MeOH, rt, 0.5 h; (c) I_2, DMSO, reflux, 4 h; (d) $SnCl_2$-HCl, MeOH, reflux, 6 h; (e) aryl aldehydes/glyoxylic acid, MeOH/MeCN, rt or reflux

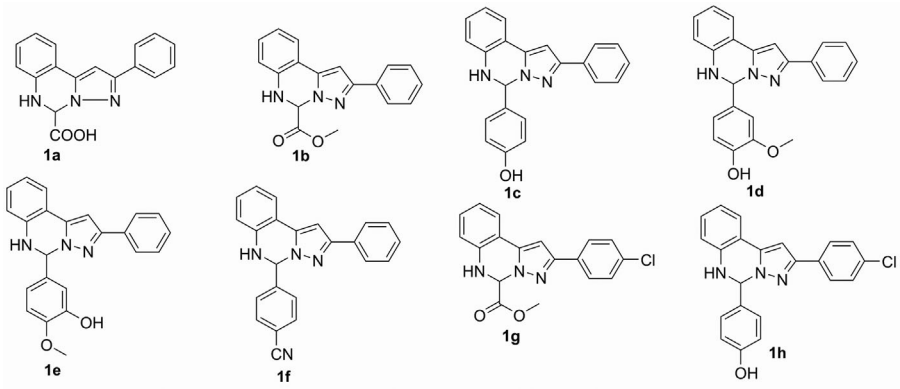

FIGURE 2 Chemical structures of the target molecules synthesized

Interestingly reaction of **6a** with glyoxylic acid performed in presence of methanol led to the formation of **1b**, a methyl ester of **1a** as a major product (**1b**; 90%), along with **8** (minor product; 10%) (Figure 3). The formation of **1b** could be due to *in situ* esterification of initially formed **1a** by MeOH (used as solvent) under non-acidic conditions. Whereas **8** was formed as a result of decarboxylation of **1a** followed by oxidation. Further, attempt to solely prepare **1a** was made successful by the reaction of **6a** with glyoxylic acid (NMR) in MeCN in 5 min at 0°C.

2.2 | Biological studies

2.2.1 | Antiproliferative activity against rat C6 glioma cells

To assess the antiproliferative potential of the synthesized compounds rat C6 glioma cells were utilized. The tumors derived from rat C6 cell implants exhibit similar morphology and vascularization grade comparable to human glioblastoma.[28] It was observed that all the investigational molecules (**1a–h**) exhibited profound antiproliferative activity (Table 1; IC_{50} < 10 μM) in rat C6 glioma cells at 48 h treatment. Two compounds **1b** and **1h** portrayed most potent cytotoxicity with IC_{50} values 3.98 and 3.86 μM, respectively, comparable to positive control etoposide (IC_{50} = 4.32 μM). In order to ascertain preferential cytotoxicity of **1b** and **1h**, normal cells, i.e., human peripheral blood mononuclear cells (hPBMCs), were treated with these compounds at 1, 5, and 25 μM concentrations. To our satisfaction no significant cytotoxicity toward hPBMCs (Figure 4) was observed, even at the highest concentration (25 μM) of tested compounds, after treatment for 48 h.

2.2.2 | Intracellular reactive oxygen species (ROS) measurement by DCFDA assay

The anticancer molecules tend to alter the intracellular ROS upon treatment.[18–20,29] In order to know exact pattern of alteration in ROS levels, rat C-6 glial cells were treated with the representative compounds **1a**, **1b**, **1d**, and **1h** for 48 h and measurements were done using DCFDA fluorescence assay. It was observed that at lower concentration (1 μM) all the test compounds showed increase in ROS production compared to normal control. The trend was reversed at higher concentration of 5 and 25 μM of the test compounds. Overall it may be concluded that all the compounds showed significant alteration in ROS levels (Figure 5).

2.2.3 | Redefining selectivity of investigational molecules (1b and 1h) as hTopoIIα inhibitors

hTopoII mediated DNA decatenation assay

Etoposide is a well-established anticancer compound that works by inhibiting TopoII enzyme. In the present study, the most potent compounds **1b** and **1h** were analyzed for inhibition of TopoII mediated decatenation in comparison to etoposide as a reference

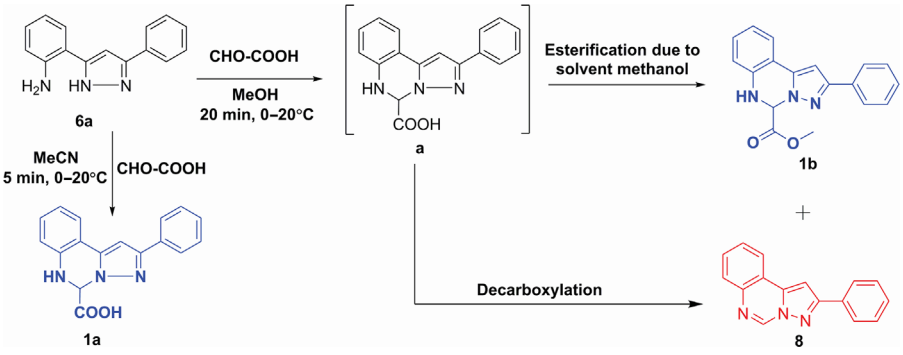

FIGURE 3 Synthesis of **1a**, **1b**, and **8**

TABLE 1 Antiproliferative activity of investigational compounds **1a–h** analyzed via MTT assay in rat-derived C6 glioma cells

Entry	Rat C6 glioma cells ± SD[a] (IC_{50}; μM)
1a	6.45 ± 0.94
1b	3.98 ± 1.35
1c	7.78 ± 1.24
1d	4.72 ± 0.97
1e	8.11 ± 1.22
1f	9.32 ± 1.76
1g	7.83 ± 1.24
1h	3.86 ± 0.98
Etoposide	4.32 ± 0.63

[a]Values are derived from averaging three independent experiments and each experiment was done in triplicate.

standard.[18,19,29] In this assay, kDNA (kinetoplast DNA), the substrate for decatenation is unable to migrate during agarose gel electrophoresis and hence remains in the agarose well itself. hTopoIIα enzyme decatenates kDNA into relatively smaller and circular form and unlike kDNA they migrate with ease inside the agarose gel during electrophoresis. Due to etoposide mediated hTopoIIα inhibition, the two forms have not been observed in the gel image (Figure 6A). Also in the presence of compounds **1** and **2**, these forms were absent and further densitometric analysis revealed significant inhibition of hTopoIIα by the investigational compounds in comparison to etoposide. Degree of inhibition among them is in the order: etoposide < **1b** < **1h** (Figure 6B).

DNA intercalation assay

A distinctive characteristic of intercalative drugs is the unwinding of DNA, e.g., ethidium bromide, AMSA, chloroquine. In gel electrophoresis, ethidium bromide (EtBr) impedes the migration of supercoiled DNA (scDNA) due to intercalative action.[30,31] **1b** and **1h** did not show any such retardation of scDNA (as observed in Figure 6C) which proves DNA non-intercalative nature of investigated compounds.[18,19,29]

2.3 | Molecular docking and prediction of physiochemical parameters

In order to theoretically investigate the binding patterns of **1b** and **1h** at TopoIIα active site, the stereoisomers of **1b** (**1b*R***, **1b*S***) and **1h** (**1h*R***, **1h*S***) were docked onto the ATPase domain of hTopoII (PDB entry: 1ZXM).[25,32] AMP-PNP in ATPase domain presented some important key amino acid interactions that include the H-bond interactions between carbonyl of ASN120 with the NH_2 of adenine moiety and between side chain residue SER149 and SER148 with —OH of ribose unit. The backbone residue interactions (GLY166, ALA167, ASN163, TYR165) and side chains residues interactions (SER148, LYS168, GLU87, ASN91, and GLN376) were observed with phosphate groups. The Mg^{++} ion exists in an octahedral geometric state having ionic interaction with the oxygen attached to the three phosphate groups. The conserved region (Walker A motif) comprising ARG162, ASN163, GLY164, TYR165, GLY166, and ALA167 helps binding of inhibitors at ATPase domain.

The binding mode of the top scoring compound, **1h*R*** (Figure 7A), revealed that the —OH group forms an H-bond interaction with —NH_2 of SER148 (3.2 Å) and THR147 (Figure 7C); and the oxygen atom of OH group interacts with ammonium ion of backbone residue LYS168 (2.8 Å). The hydroxy benzene ring showed π–cation interactions with Mg^{++} 903 (3.2 Å). The π–cation interaction was also observed between ARG98 and aromatic ring attached quinazoline ring. The NH of the quinazoline ring formed a hydrogen bond with the SER149. The compound **1h** (***R***), however, has shown hydrophobic interactions with ILE217 and polar interactions with THR215 and ASN91 (Figure 7). The overall binding pattern of compounds **1h*R*** and **1b*R*** were found to be similar as of AMP-PNP (Figure 7B).

The compounds **1b** and **1h** were predicted for their pharmaceutically relevant properties such as blood brain barrier, partition coefficient, bioavailability, pharmacokinetics, etc. using QikProp module in MAESTRO 11.4.[33] The indispensable lead generation and optimization property of the module suggested that **1b** and **1h** have blood brain barrier coefficient (QPlogBB) of −1.68 and −2.09, respectively (range: −3.0 to 1.2), and can cross blood brain barrier. Moreover, the partition coefficient (QPlogPo/w) predicted was in the normal range i.e., −2.0 to 6.5. QPPCaco represents the gut cell absorption of the compounds ranges from 25 for poor gut absorbed

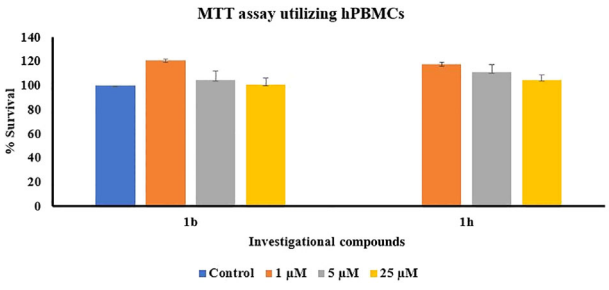

FIGURE 4 Effect of cytotoxity by compounds **1b** and **1h** on hPBMC. No cytotoxicity was found up to 25 μM at 48 h

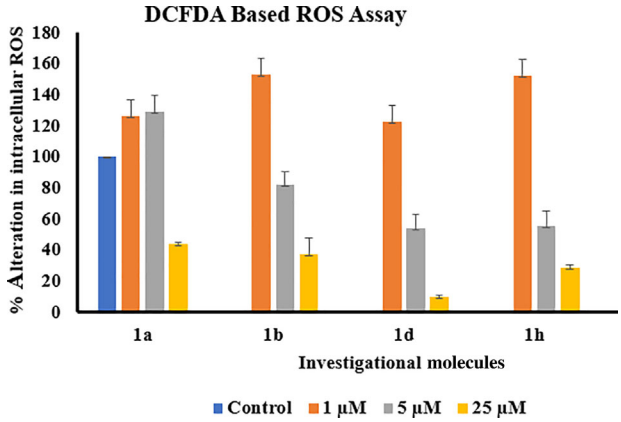

FIGURE 5 Percent alteration in intracellular ROS levels in rat C6 glial cells in response to treatment with synthesized compounds at concentrations of 1, 5, and 25 μM at 48 h. Measured via DCFDA assay

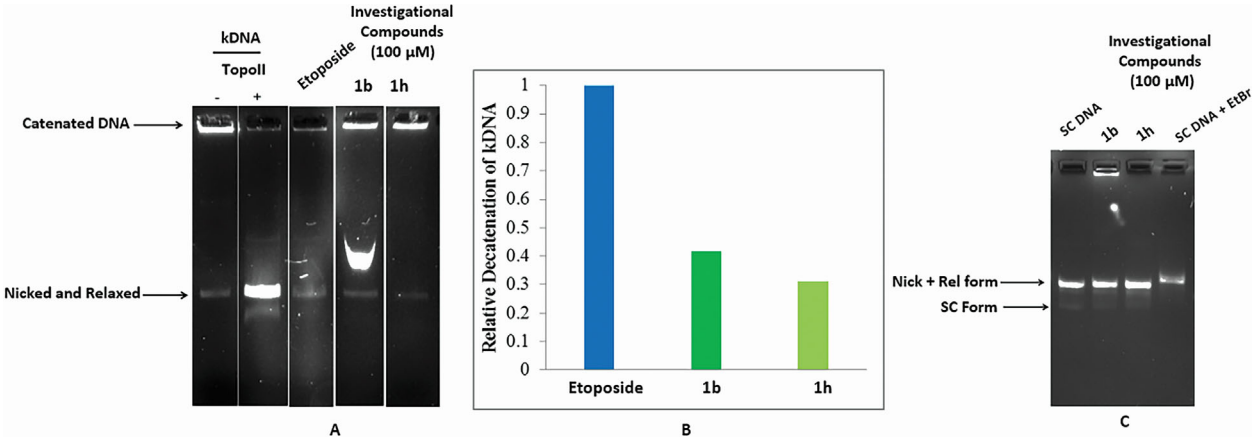

FIGURE 6 (A) Agarose gel image for decatenation assay: kDNA and hTopoIIα were incubated in presence and absence of 100 µM etoposide (E) and investigational compound **1b** and **1h** (100 µM). (B) Relative decatenation of kDNA by investigational compounds **1b** and **1h** in comparison to etoposide after quantification. (C) Agarose gel image for DNA intercalation assay. Supercoiled DNA (pUC 19 plasmid) was incubated in the presence and absence of ethidium bromide (final concentration 1 µg/mL) and investigational compounds **1b** and **1h**

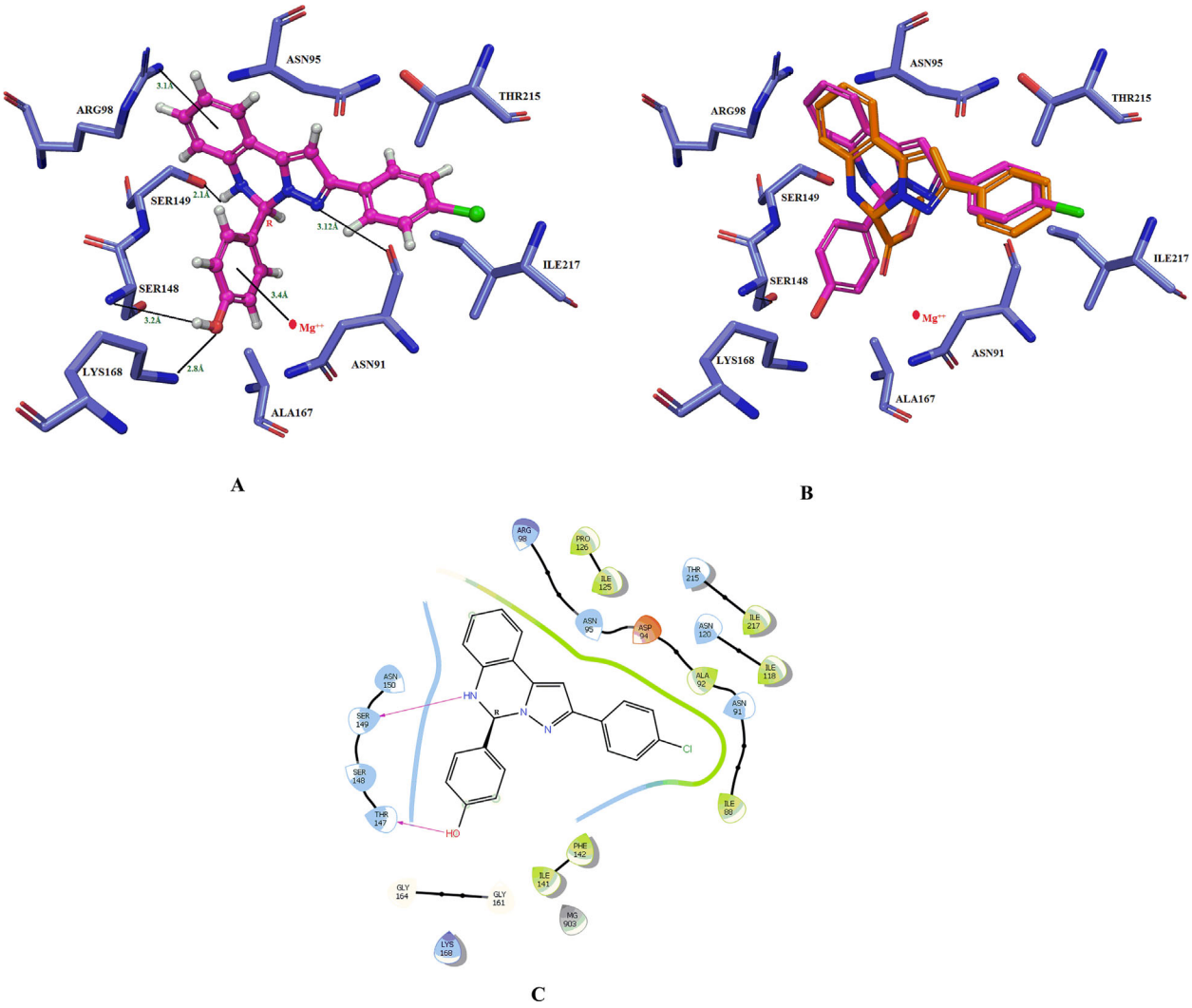

FIGURE 7 (A) 3D Binding mode of **1h*R*** at the ATPase domain of topoisomerase II. (B) Docked compounds **1h*R*** (pink) and **1b*R*** (orange) at ATPase domain of topoisomerase II. (C) 2D interaction diagram of **1h*R*** in hTopoIIα

TABLE 2 Important physiochemical properties of the compounds that help in the drug penetrance to brain, gut and oral absorption

Entry	Compound number	QPlogPo/w	QPPCaco	QPlogBB	Human oral absorption
1	**1b**	3.845	2061.737	−0.209	3
2	**1h**	5.268	1663.569	−0.144	1

compounds while >500 for the compounds with good gut absorption. The human oral absorption depends on the number of rotatable bonds, number of metabolites, logP, cell permeability, and solubility. The number 1 depicts low oral absorption, 2 represents medium oral absorption, and 3 represents high oral absorption. Compound **1h** was predicted to have low human oral absorption as compared to **1b** (Table 2).

2.4 | Cell cycle analysis and prediction of mode of cell death

2.4.1 | Cell cycle analysis

The inhibition of specific target by the anticancer compounds tend to cause cell death and halt the cell cycle progression[24] by arresting cell cycle.[18–20,29] To investigate the specific phase of cell cycle arrested by our investigational compounds (**1b**, **1h**), rat C6 glioma cells were utilized and treatment was given at two concentrations, 5 and 25 μM for 24 h. The results showed significant changes in G1 pattern (33.59% in control, 87.06% in **1b**, 82.21% in **1h**) treated at 5 μM concentration. The compounds at 25 μM induced increase in sub-G1 population several folds (82.21–87.06%) indicative of cell death. This peculiar feature may be attributed to the fact that compounds may be toxic to the glioma cells independent of the status of cell cycle or cells might be having mitotic catastrophy[20] at the higher drug concentration (Figure 8).

2.4.2 | Prediction of cell death mode

To examine the mode of cell death, we performed annexin-V versus propidium iodide staining utilizing the investigational compounds **1b** and **1h**, at 5 and 25 μM concentration. The assay is based on the principle that annexin-V binds to the apoptotic populations (detects the release of phosphatidylserine) under normal conditions whereas propidium iodide does not stain live or early/late apoptotic cells. In late apoptotic and necrotic cells, the integrity of the plasma and nuclear membranes declines allowing propidium iodide to pass through the membranes which further intercalate with nucleic acids and display red fluorescence.[18–20,29] Compounds **1b** and **1h** induced early apoptosis at 5 μM and the mode of cell death was late apoptosis at 25 μM (Figure 9).

3 | CONCLUSION

In summary, we have designed, synthesized, and evaluated the dihydropyrazolo[1,5-*c*]quinazolines (**1a**–**h**) as inhibitors of rat C6-glioma cells. The most potent inhibitors **1b** and **1h** were found to be

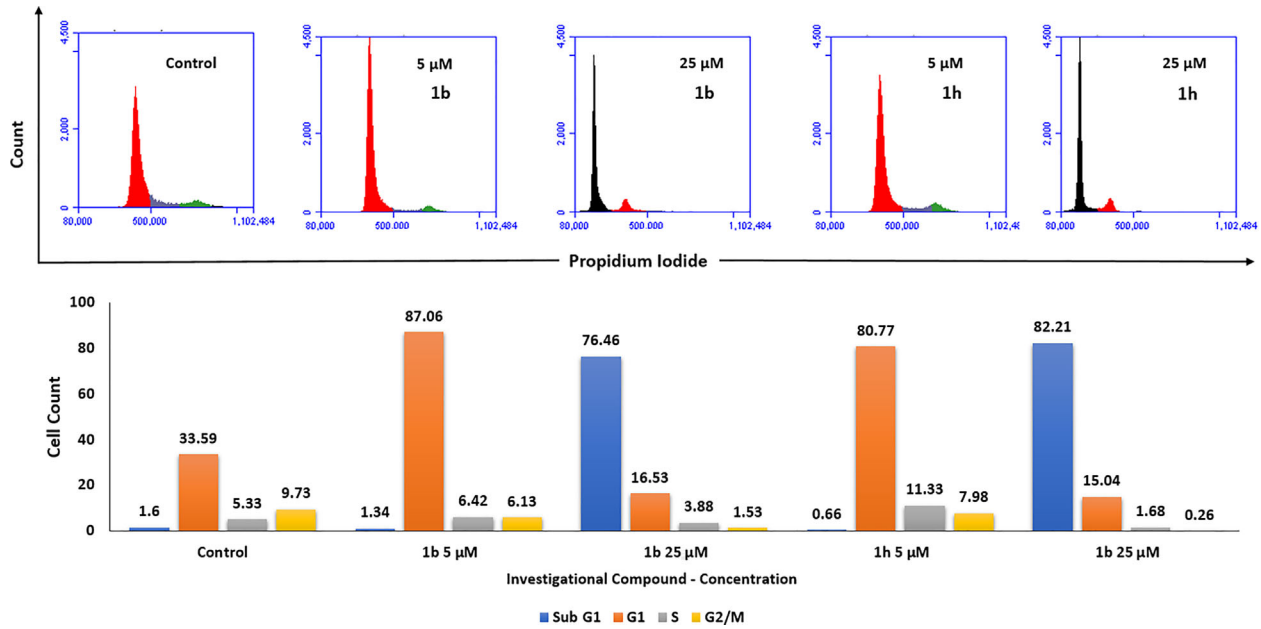

FIGURE 8 Cell cycle analysis using propidium iodide. Rat C6 glioma cells were treated with **1b** and **1h** at 5 and 25 μM concentration. The bar graph represents the percent cell count (DNA) at various stages of cell cycle induced by investigational compounds

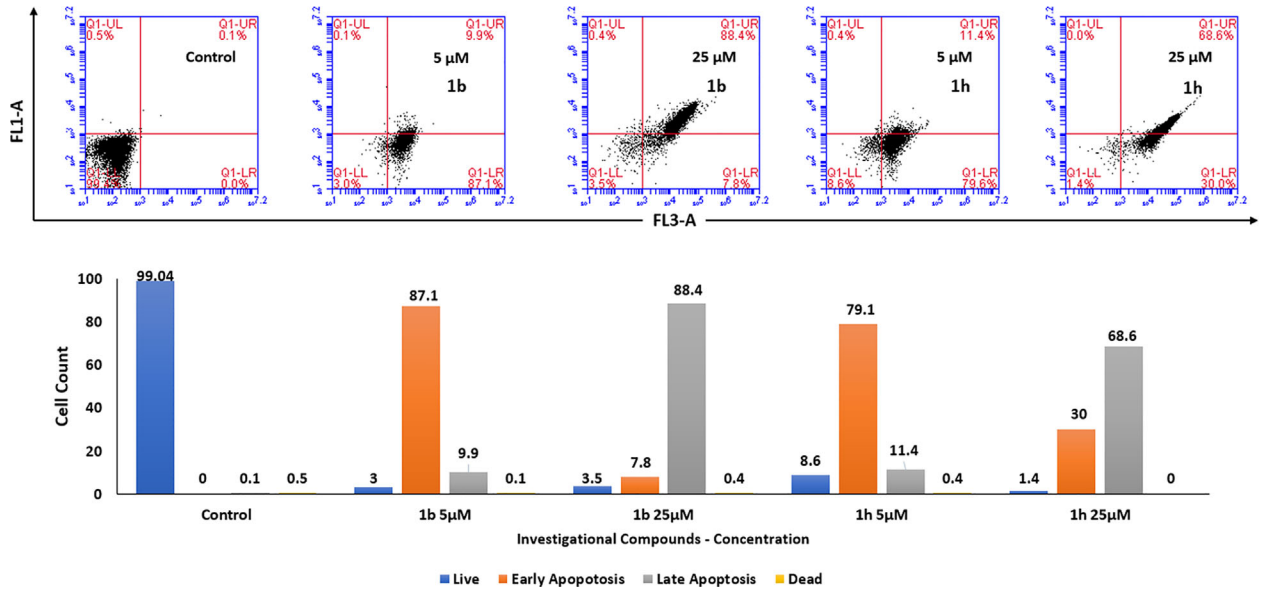

FIGURE 9 Mode of cell death prediction by PI versus annexin V assay. The investigational compounds **1b** and **1h** exhibited rat C6 glioma cell death via apoptosis

non-cytotoxic toward normal cells (HPBMCs) at highest concentration. The compounds were able to alter the intracellular ROS levels and inhibited TopoII which was further corroborated through *in silico* studies. Compounds delayed cell cycle, caused G1 phase arrest at low concentration and induced apoptosis at higher concentration. All the above annotations indicated multiple modes of mechanisms involved in anticancer effects of compounds. Further results on their detailed antitumor potential and effect of receptor inhibition of down targets, formulation and SAR will be published in due course of time. The experiments were conducted in accordance to protocol no. CUPB/cc/14/IEC/4483 approved by Institutional Ethics Committee of Central University of Punjab, Bathinda, as per guidelines issued by Indian Council of Medical Research (ICMR), Govt. of India.

4 | EXPERIMENTAL

4.1 | Chemistry

4.1.1 | General

All the chemical and biological reagents were purchased from Sigma–Aldrich, Loba-Chemie Pt. Ltd., S.D. Fine Chemicals, Sisco Research Laboratory, and Avra Synthesis Ltd. and were used without further purification. Sartorius analytical balance (BSA224S-CW) and Mettler Toledo were used for the weighing purposes. JSGW heating mantle, Tarson spinot digital, ILMVAC digital rotary evaporater, digital hop top, and NSW oven/vacuum oven were used during reaction. TLC monitored the progress of the reaction, using *n*-hexane/ethyl acetate and chloroform/methanol as the mobile phase on pre-coated Merck TLC (TLC silica gel 60, F254) plates in JSGW UV/fluorescent analysis cabinet and/or iodine chamber. Melting points were recorded on Stuart melting point apparatus (SMP-30) with open glass capillary tubes and were uncorrected. Infrared (IR) spectra of compounds were recorded with KBr on a Bruker FT-IR spectrophotometer. ^{1}H and ^{13}C nuclear magnetic resonance (NMR) spectra were recorded at Panjab University, Chandigarh in $CDCl_3$/d_6-DMSO on a Bruker Avance II (400 MHz) NMR spectrometer using TMS ($\delta = 0$) as an internal standard. Mass spectra were recorded on TOF-MS/ESI at Panjab University, Chandigarh and MS/EI at Central University of Punjab, Bathinda.

The NMR spectra of compounds **1a**,**b** and the InChI codes of the investigated compounds together with some biological activity data are provided as Supporting Information.

4.1.2 | General procedure for the synthesis of chalcones 3a,b

A mixture of 2-nitrobenzaldehyde (1 mmol) and appropriate aryl ketone (1 mmol) in glacial acetic acid was stirred in 100 mL round bottomed flask (RBF). Conc. sulfuric acid (4–5 drops) was added to the reaction mixture in ice cold condition and further stirred at room temperature for 24 h. Completion of the reaction was determined by thin layer chromatography (TLC). After the completion, the reaction mixture was poured on ice-cold water and filtered. The solid was washed with water and dried to obtain the crude product. The crude product was recrystallized from methanol to get pure compound.[19,26,27]

Physical data of the representative compound 3a

Yield: 85%, 142.37 mg, creamy white solid, mp: 89–91°C; IR (KBr, cm^{-1}): 1666 (C═O), 1610 (C═C), 1510 (N═O), 1342 (N═O), 1014 (C—N). ^{1}H NMR ($CDCl_3$, 400 MHz): 8.12 (1H, d, J = 15.9 Hz), 8.02 (3H, bs), 7.69–7.74 (2H, m), 7.50–7.57 (4H, m), 7.34 (1H, d,

J = 15.9 Hz).^{13}C NMR ($CDCl_3$, 75 MHz): 190.22, 148.34, 140.03, 137.20, 133.56, 133.09, 131.08, 130.31, 129.13, 128.62, 126.97, and 124.86.

4.1.3 | General procedure for the synthesis of pyrazolines 4a,b

To a solution of appropriate chalcone (1 mmol) in methanol (5 mL) was added hydrazine hydrate (2 mmol). The reaction mixture was stirred for 2 h. After completion of the reaction (TLC), precipitate formed was filtered and washed with excess methanol to obtain the pure product **4a** and **4b**.[26,27]

Physical data of the representative compound 4a

Yield: 97%, 102.3 mg, orange crystalline solid, mp: 140–142°C IR (KBr, cm^{-1}): 3310 (N—H stretch), 1575 (N—H bend), 1517 (N═O), 1350 (N═O), 1605 (C═N), 1056 (C—N); ^{1}H NMR ($CDCl_3$, 400 MHz): 7.96 (2H, t, J = 8.4 Hz), 7.65 (3H, m), 7.41 (4H, m), 6.05 (D_2O exchangeable NH, 1H, s), 5.42 (1H, t, J = 13.2 Hz), 3.80, (1H, m), 3.01 (1H, m).

4.1.4 | General procedure for the synthesis of pyrazoles 5a,b

To a solution of appropriate pyrazolines (**4a**,**b**) in DMSO was added catalytic amount of molecular iodine and reaction mixture was refluxed at 130–140°C for 4–6 h. After the completion of the reaction (TLC), the reaction mixture was poured in ice cold water; solid product was extracted using ethyl acetate. Excess iodine was removed adding aq. sodium thiosulfate. Organic layer was washed with brine (10 mL × 3), dried over sodium sulfate, and was finally evaporated under reduced pressure using rotary evaporator to obtain the product (**5a**,**b**).[26,27]

Physical data of the representative compound 5a

Yield: 92%, 91.31 mg, brownish solid, mp: 194–196°C IR (KBr, cm^{-1}): 3456 (N—H stretch), 1664 (C═C), 1620 (C═N), 1524 and 1348 (N═O), 1144 (C—N). ^{1}H NMR ($CDCl_3$, 400 MHz): 7.67–7.76 (3H, m), 7.56–7.63 (3H, m), 7.33–7.51 (5H, m). ^{13}C NMR ($CDCl_3$, 100 MHz): 149.02, 146.37, 146.16, 132.09, 130.97, 129.04, 128.74, 128.04, 126.47, 125.62, 124.56, 123.82, and 102.59.

4.1.5 | General procedure for reduction of 2-nitropyrazoles 5a,b to their aniline derivatives 6a,b

To a mixture of **5a** and **5b** in methanol was added $SnCl_2$ (3–4 equivalents). The reaction mixture was refluxed for 4 h. After the completion of the reaction (TLC), methanol was evaporated under reduced pressure using rotary evaporator. Solid product was than extracted with ethyl acetate (10 mL × 3). Excess of $SnCl_2$ was precipitated in water by neutralizing the reaction mixture with 5% NaOH. Organics were washed with brine (10 mL × 3), dried over anhydrous Na_2SO_4, and evaporated under reduced pressure using rotary evaporator to obtain the final product **6a**,**b**.[26,27]

Physical data of the representative compound 6a

Yield: 95%, 88.24 mg, yellow solid, mp: 165–166°C; IR (KBr, cm^{-1}): 3360 (N—H), 3285 (N—H), 1613 (C═N), 1579 (CC), 1248 (C—N). ^{1}H NMR ($CDCl_3$, 400 MHz): 13.23 (D_2O exchangeable NH, 1H, bs), 7.81 (1H, s), 7.79 (1H, s), 7.31–7.54 (4H, m), 7.00 (2H, s), 6.75 (1H, d, J = 7.91 Hz), 6.61 (1H, t, J = 7.32 Hz), 6.22 (D_2O exchangeable NH, 2H, bs).

4.1.6 | Synthesis of 2-phenyl-5,6-dihydropyrazolo[1,5-*c*]quinazoline-5-carboxylic acid (1a)

To a solution of **6a** (0.1 g, 0.4255 mmol) in acetonitrile was added glyoxylic acid (31.4 mg, 0.4355 mmol) (50% aqueous soln) and mixture was stirred at 10–15°C for 5 min. After the completion of reaction (TLC), reaction mixture was evaporated using rotary evaporator and solid product was obtained. The compound was further purified using flash chromatography to obtain **1a**.

Yield: 98%, creamy white solid, mp: 190–192°C. ^{1}H NMR ($CDCl_3$, 400 MHz, δ with TMS = 0): 12.4 (1H, s), 7.84 (2H, d, J = 7.29 Hz), 7.51 (1H, d, J = 7.16 Hz), 7.38–7.45 (4H, bs), 7.30 (1H, m), 7.11 (1H, m), 7.04 (1H, s), 6.90 (1H, d, J = 8 Hz), 6.80 (1H, m), 6.01 (1H, d). ^{13}C NMR ($CDCl_3$, 100 MHz, δ with TMS = 0): 169.75, 151.07, 139.43, 138.34, 132.95, 129.07, 128.09, 127.57, 125.14, 123.65, 118.53, 114.75, 112.84, 96.49, and 68.41. Anal. calcd. for $C_{17}H_{13}N_3O_2$: C, 70.09; H, 4.50; N, 14.42. Found: C, 70.15; H, 4.62; N, 14.39.

4.1.7 | Synthesis of methyl 2-phenyl-5,6-dihydropyrazolo[1,5-*c*]quinazoline-5-carboxylate

To a solution of **6a** (0.1 g, 0.4255 mmol) in methanol was added glyoxylic acid (31.4 mg, 0.4355 mmmol) (50% aqueous solution) and stirred at 10–15°C for 5 min. After the completion of reaction (TLC), reaction mixture was evaporated using rotary evaporator and solid product was obtained. The compound was further purified using flash chromatography to obtain **1b**.

^{1}H NMR ($CDCl_3$, 400 MHz): 7.84 (2H, d, J = 5.8 Hz), 7.51 (1H, d, J = 6.4 Hz), 7.40 (2H, s), 7.32 (1H, d, J = 6.16 Hz), 7.14 (1H, s), 7.04 (1H, s), 6.88 (3H, t, J = 10 Hz), 6.11 (1H, s), 3.67 (3H, s). ^{13}C NMR ($CDCl_3$, 100 MHz): 168.40, 151.56, 138.43, 138.19, 132.51, 128.91, 128.05, 127.38, 125.05, 123.98, 123.36, 118.86, 114.70, 96.17, 68.08, and 52.13. Anal. calcd. for $C_{18}H_{15}N_3O_2$: C, 70.81; H, 4.95; N, 13.76. Found: C, 70.97; H, 5.08; N, 14.11.

4.1.8 | Synthesis of 4-(2-phenyl-5,6-dihydropyrazolo[1,5-*c*]quinazolin-5-yl)phenol (1c)

A mixture of **6a** (0.1 g, 0.425 mmol) and 4-hydroxybenzaldehyde (0.70 g, 0.425 mmol) was dissolved in methanol and refluxed for 1 h. After the completion of the reaction (TLC), the reaction mixture was left to cool. Precipitated solid was obtained by decanting extra methanol and recrystallized from methanol to obtain **1c**.[26,27]

4.1.9 | Synthesis of 2-methoxy-4-(2-phenyl-5,6-dihydropyrazolo[1,5-*c*]quinazolin-5-yl)phenol (1d)

A mixture of **6a** (100 mg, 0.425 mmol) and 4-hydroxy, 3-methoxy benzaldehyde (64.6 mg, 0.425 mmol) was dissolved in methanol and refluxed for 1 h. After the completion of the reaction (TLC), the reaction mixture was left to cool. Precipitated solid was obtained by decanting extra methanol and recrystallized from methanol to obtain **1d**.[26,27]

4.1.10 | Synthesis of 2-methoxy-5-(2-phenyl-5,6-dihydropyrazolo[1,5-*c*]quinazolin-5-yl)phenol (1e)

A mixture of **6a** (100 mg, 0.425 mmol) and 4-hydroxybenzaldehyde (64.6 mg, 0.425 mmol) was dissolved in methanol and refluxed for 1 h. After the completion of the reaction (TLC), the reaction mixture was left to cool. Precipitated solid was obtained by decanting extra methanol and recrystallized from methanol, to obtain **1e**.[26,27]

4.1.11 | Synthesis of 4-(2-phenyl-5,6-dihydropyrazolo[1,5-*c*]quinazolin-5-yl)benzonitrile (1f)

A mixture of **6a** (100 mg, 0.425 mmol) and 4-cyanobenzaldehyde (55.67 mg, 0.425 mmol) was dissolved in methanol and refluxed for 1 h. After the completion of the reaction (TLC), the reaction mixture was left to cool. Precipitated solid was obtained by decanting extra methanol and recrystallized from methanol to obtain **1f**.[26,27]

4.1.12 | Synthesis of methyl 2-(4-chlorophenyl)-pyrazolo[1,5-*c*]quinazoline-5-carboxylate (1g)

To a solution of **6b** (0.1 g, 0.371 mmol) in methanol was added glyoxylic acid (0.042 mL, 0.371 mmol) (50% aqueous soln) at 10–15°C. The reaction mixture was stirred for 5 min. After the completion of reaction (TLC), reaction mixture was evaporated using rotary evaporator and solid mixture of products was obtained which was further purified by column chromatography to obtain **1g**.

Yield: 60%, creamish white, mp: 215–217°C. ^{1}H NMR ($CDCl_3$, 400 MHz): 7.80–7.75 (2H, m), 7.52 (1H, dd, *J* = 7.72 Hz), 7.38 (2H, dd, *J* = 6.72 Hz), 7.26 (1H, d, *J* = 5.52 Hz), 7.00 (1H, s), 6.95 (1H, d, *J* = 7.76 Hz), 6.83 (1H, d, *J* = 7.52 Hz), 6.00 (1H, d, *J* = 1.92 Hz), 4.98 (D_2O exchangeable NH, 1H, s), 3.68 (3H, s). ^{13}C NMR (CDC_{l3}, 100 MHz): 169.18, 151.71, 138.64, 138.04, 135.95, 133.80, 131.59, 129.69, 128.82, 127.15, 120.93, 115.56, 114.09, 97.29, 68.79, and 53.22. Anal. calcd. for $C_{18}H_{14}ClN_3O_2$: C, 63.63; H, 4.15; Cl, 10.43; N, 12.37. Found: C, 63.02; H, 4.34; N, 12.56.

4.1.13 | Synthesis of 4-(2-(2-chlorophenyl)-5,6-dihydropyrazolo[1,5-*c*]quinazolin-5-yl)phenol (1h)

A mixture of **6b** (0.1 mg, 0.371 mmol) and 4-hydroxybenzaldehyde (0.45 mg, 0.371 mmol) was dissolved in methanol and refluxed for 1 h. After the completion of the reaction (TLC), the reaction mixture was left to cool. Precipitated solid was obtained by decanting extra methanol and recrystallized from methanol to obtain **1h**.[26,27]

4.2 | Biological assays

4.2.1 | Cell culture and treatment

Rat C6 glioma cells were generously gifted by Prof. Gursharan Kaur, GNDU, Amritsar, India. They were grown in DMEM media containing 10% FBS, 100 units/mL penicillin, and 100 µg/mL streptomycin and were maintained at 37°C in a 5% CO_2 humidified incubator. When the cells became 70–80% confluent, culture medium was removed and discarded. Then the cells were rinsed with PBS to remove all the traces of serum that contains trypsin inhibitor. After that, trypsin-EDTA 0.25% (w/v) solution was added to the flask. It was then allowed to incubate until cells were detached from the surface (trypsinization). Subsequently, trypsin was inactivated by the addition of media containing serum (1 mL). Centrifugation was done on 1200 rpm at 37°C for 10 min for harvesting the cells. Further, supernatant was disposed and resuspension of the cell pellet was done using 2 mL of the media. The cell number was counted using automated cell counter. The cells were transferred to fresh media every 3 days. The maintenance of C6 cultured cell line was done in 25 or 75 cm^2 flasks containing DMEM medium supplemented with 10% FBS, 1× antibiotic solution and afterward incubated at 37°C in a humidified atmosphere containing 5% CO_2 and 95% humidity.[18–20,29]

The cells were seeded in 25 cm^2 flasks and the treatment was given when 70–80% confluency was obtained. The treatment time of different test compounds was as described earlier in the section 2.

Similarly, HPBMC culture was done as per previous published protocol.[18–20] A total of 5 mL of fresh blood was drawn from healthy individual as per the protocol no. CUPB/cc/14/IEC/4483 approved by Institutional Ethics Committee of Central University of Punjab, Bathinda. The protocol used was standard operating procedure, provided by Institutional Ethics Committee of Central University of Punjab according to guidelines issued by Indian Council of Medical Research (ICMR), Govt. of India.

4.2.2 | Evaluation of anti-proliferative activity of the synthesized compounds (MTT assay)

Rat C6 glial cells were counted on the automated cell counter. About 8000–10000 cells were seeded in each well of the 96 well plates. The plate was incubated at 37°C with 5% CO_2 for 24 h. At the end of the 24 h, treatment was given to the cells in concentrations of 1, 5, and 25 µM. The cells were further incubated for 48 h. The media was removed from each well and MTT solution (5 mg/10 mL) was added. This was incubated in the dark for 4 h. At the end of 4 h, the MTT solution was disposed from each well and the intracellular precipitate was dissolved in DMSO solution and the absorbance was read at 570 nm using a microplate reader (BioTek).[18–20,29]

4.2.3 | Intracellular ROS measurement by DCFDA assay

The treated and control rat C6 glial cells (1×10^5), cultured in 96-well plates were equilibrated in PBS and incubated in the dark for 30 min with 100 µM of H_2DCF-DA (Invitrogen) [$Ex_{478\,nm}/Em_{518\,nm}$]. After washing twice with PBS, fluorescence was then read at the excitation wavelength of 478 nm and emission wavelength of 518 nm using BioTek Microplate Reader as per the protocol described.

4.2.4 | Topoisomerases assays for investigational compounds

hTopoIIα mediated activity in the presence of investigational compounds were probed using commercially available assay kit procured from TopoGEN, Inc., USA.

hTopoII mediated DNA decatenation assay

For this assay, reaction components such as freshly prepared 5 × buffer, 150 ng of kDNA (substrate), 100 µg drug or test compound (previously dissolved in DMSO solvent), 2 units of hTopoIIα enzyme, assay buffer and nuclease free water were added sequentially in a 1.5 mL sterile centrifuge tube. Nuclease free water was added to this reaction mixture to adjust the final reaction volume to 20 µL. Assay buffer was prepared by mixing buffer A (0.5 M Tris-HCl of pH 8, 1.5 M sodium chloride, 100 mM magnesium chloride, 5 mM dithiothreitol, 300 mg bovine serum albumin) and buffer B (20 mM ATP in water) in 1:1 ratio. The reaction mixture was incubated in a water bath at 37°C for 30 min. Reaction was stopped by adding (SDS) sodium dodecyl sulfate (final concentration 0.10% w/v) and proteinase K (final concentration 0.1 mg/mL). The catenated and decatenated forms of kDNA were analyzed by agarose gel (1% w/v) electrophoresis in 1× Tris-acetate-EDTA (TAE) running buffer containing ethidium bromide (final concentration 0.5 µg/mL) at 3.5 V/cm for 1 h 20 min. Gel was destained in water till the bands were sufficiently visible for imaging. Gel image was taken using GelDoc EZ imager (BioRad™) and quantitated by Image lab software.

DNA intercalation assay

For this assay, 150 ng of scDNA was incubated with EtBr and investigational compounds **1b** and **1h** at 37°C for 20 min. The reactions were analyzed by 1% w/v agarose gel electrophoresis in 1× TAE running buffer at 3.5 V/cm for 30 min. After electrophoresis, gel was first stained with EtBr solution for 30 min and later destained with water for sufficient time till the bands were sufficiently visible for imaging. Gel image was taken using Gel Doc EZ imager (BioRad™).

4.3 | Molecular docking methodology

3-Diminesional co-crystal structure of hTopoIIα with ATP was retrieved from Protein Data Bank (PDB 1ZXM) and was further edited for protein preparation by removing excess crystallized water molecules, chains (using PyMol visualizer). The protein preparation was done using protein preparation wizard of maestro 11.4. The protein was preprocessed for the addition of the polar hydrogens, cysteine bridges creation, charges, filling missing side chains, etc. This preprocess step also corrects the ionization and tautomeric states of amino acid residues and therefore modifies the total Gasteiger charges on the protein structure. The optimization of the interactions between the side chains and ligand with side chains was done. The energy minimization of the X-ray structure was done at the RMSD value of 0.3 Å. This energy minimization also ensures the placement of hydrogen atoms in an optimized geometry. Chemical structures of ligands were drawn in ChemDraw professional and minimized by using OPLS3 force-field (LigPrep module) where 1000 iteration cycles were run, to get the steepest energy minimized structure. The Grid was generated with the aid of Receptor grid generation module, which is a user defined three-dimensional grid particular selecting the residues of ATPase domain for docking. In the present study, the location and dimensions of the grid box was taken from the coordinates of the centroid of the already embedded ATP molecule, with the help of Maestro visualizer. Each docking experiment was done by implicating the Lamarckian Genetic Algorithm (LGA) which was set with the total 1000 conformations, 50 different runs with termination after 250000 energy evaluation. Population size was set out to be 150. Finally, the conformation of lowest predicted binding free energy of the most occurring binding modes in the hTopoIIα active pocket was selected.

4.4 | Cell cycle analysis

Cellular samples (C6 previously treated with investigational compounds **1b** and **1h** for 48 h and control) were prepared for staining by propidium iodide (PI). The standard protocol set up by our laboratory was utilized for the analysis.[18–20,29] The cells approximately 10^6 were trypsinized and transferred to each tube. The cells were further centrifuged at 1200 rpm for 5 min and washed with 1× PBS. Thereafter cells were fixed using chilled methanol and incubated for 3 h at −20°C. Post 3 h, cells were subjected to centrifugation at 2500 rpm and washed once with 1× PBS. A total of 50 µL of propidium iodide (along with 50 µL ribonuclease A) was added to each well and incubated for 30 min at room temperature in dark. The DNA content was then measured using flow cytometer (BD Accuri).

4.5 | Prediction of mode of cell death

For predicting whether the cell death induced by investigational compounds (**1b** and **1h**) is apoptosis or necrosis PI versus Annexin V assay was done. The assay was conducted in accordance to our previously reported laboratory protocols.[18–20,29] C6 cells previously treated with investigational compounds (**1b** and **1h**) for 48 h were trypsinized and were centrifuged at 1200 rpm for 5 min and washed with 1× PBS. The cellular samples (approx. 10^6 cells in each tube) were taken and stained with Annexin V and PI dye (50 µL each dye for each sample). The samples were incubated for 30 min at room temperature in the dark and mode of cell death was analyzed using flow cytometer (BD Accuri).

4.6 | hPBMC culture and MTT assay

hPBMCs were obtained from whole blood after treatment with RBC lysis buffer and were then suspended in RPMI media supplemented with 10% fetal bovine serum (FBS), 1× antibiotic solution and were incubated at 37°C with 5% CO_2 and 95% humidity. The PBMCs were counted on the automated cell counter (Invitrogen). MTT assay was done as mentioned under section 4.2.2.

ACKNOWLEDGMENTS

RK, GJ, and SK are thankful to Central University of Punjab and Bristol-Myer Squibb, USA [Grant No. 34003085] for providing infrastructure and funds.

CONFLICT OF INTEREST

Authors declare no conflict of interest.

ORCID

Raj Kumar http://orcid.org/0000-0001-5113-6627

REFERENCES

[1] J. C. Wang, *Nat. Rev. Mol. Cell. Biol.* **2002**, *3*, 430.
[2] R. Kumar, S. Singh, *Topoisomerase Inhibitors: Classification, Mechanisms of Action and Adverse Effects*. Nova Publications, New York, USA **2017**.
[3] Y. Pommier, E. Leo, H. Zhang, C. Marchand, *Chem. Biol.* **2010**, *17*, 421.
[4] A. Singh, N. Kaur, G. Singh, P. Sharma, P. Bedi, S. Sharma, K. Nepali, *Recent Pat. Anticancer Drug Discov.* **2016**, *11*, 401.
[5] S. M. Cuya, M.-A. Bjornsti, R. C. van Waardenburg, *Cancer Chemother. Pharmacol.* **2017**, *80*, 1.
[6] C. Bailly, *Chem. Rev.* **2012**, *112*, 3611.
[7] J. L. Nitiss, *Nat. Rev. Cancer* **2009**, *9*, 338.
[8] H. Zhao, H. Yu, Y. Liu, Y. Wang, W. Cai, *Clin. Neuropathol.* **2008**, *27*, 83.
[9] V. Vinson, *Science* **2017**, *355*, 257.
[10] C. M. Das, D. Aguilera, H. Vasquez, P. Prasad, M. Zhang, J. E. Wolff, V. Gopalakrishnan, *J. Neurooncol.* **2007**, *85*, 159.
[11] D.M. -T. Ho, C.-Y. Hsu, L.-T. Ting, H. Chiang, *Am. J. Clin. Pathol.* **2003**, *119*, 715.
[12] M. Binaschi, F. Zunino, G. Capranico, *Stem Cells* **1995**, *13*, 369.
[13] N. DArcy, B. Gabrielli, *Curr. Med. Chem.* **2017**, *24*, 1504.
[14] Y. Pommier, *Nat. Rev. Cancer* **2006**, *6*, 789.
[15] K. R. Hande, *Update Cancer Therapeut.* **2008**, *3*, 13.
[16] Y. Pommier, *ACS Chem. Biol.* **2013**, *8*, 82.
[17] B. Dwarakanath, D. Khaitan, R. Mathur, *Indian J. Exp. Biol.* **2004**, *42*, 649.
[18] M. Chauhan, G. Joshi, H. Kler, A. Kashyap, S. M. Amrutkar, P. Sharma, K. D. Bhilare, U. C. Banerjee, S. Singh, R. Kumar, *RSC Adv.* **2016**, *6*, 77717.
[19] G. Joshi, S. M. Amrutkar, A. T. Baviskar, H. Kler, S. Singh, U. C. Banerjee, R. Kumar, *RSC Adv.* **2016**, *6*, 14880.
[20] G. Joshi, H. Nayyar, S. Kalra, P. Sharma, A. Munshi, S. Singh, R. Kumar, *Chem. Biol. Drug Des.* **2017**, *90*, 995.
[21] G. Kaur, R. P. Cholia, A. K. Mantha, R. Kumar, *J. Med. Chem.* **2014**, *57*, 10241.
[22] G. Joshi, P. K. Singh, A. Negi, A. Rana, S. Singh, R. Kumar, *Chem. Biol. Interact.* **2015**, *240*, 120.
[23] A. T. Baviskar, U. C. Banerjee, M. Gupta, R. Singh, S. Kumar, M. K. Gupta, S. Kumar, S. K. Raut, M. Khullar, S. Singh, *Biorg. Med. Chem.* **2013**, *21*, 5782.
[24] S. Kalra, G. Joshi, A. Munshi, R. Kumar, *Eur. J. Med. Chem.* **2017**, *142*, 424.
[25] H. Wei, A. J. Ruthenburg, S. K. Bechis, G. L. Verdine, *J. Biol. Chem.* **2005**, *280*, 37041.
[26] D. Kumar, G. Kaur, A. Negi, S. Kumar, S. Singh, R. Kumar, *Bioorg. Chem.* **2014**, *57*, 57.
[27] D. Kumar, R. Kumar, *Tetrahedron Lett.* **2014**, *55*, 2679.
[28] J. M. Gunnersen, V. Spirkoska, P. E. Smith, R. A. Danks, S. S. Tan, *Glia* **2000**, *32*, 146.
[29] R. P. Cholia, S. Kumar, M. Kaur, R. Kumar, M. Dhiman, A. K. Mantha, *Metab. Brain Dis.* **2017**, *32*, 1705.
[30] R. Palchaudhuri, P. J. Hergenrother, *Curr. Opin. Biotechnol.* **2007**, *18*, 497.
[31] G. Priyadarshani, S. Amrutkar, A. Nayak, U. C. Banerjee, C. N. Kundu, S. K. Guchhait, *Eur. J. Med. Chem.* **2016**, *122*, 43.
[32] R. A. Friesner, R. B. Murphy, M. P. Repasky, L. L. Frye, J. R. Greenwood, T. A. Halgren, P. C. Sanschagrin, D. T. Mainz, *J. Med. Chem.* **2006**, *49*, 6177.
[33] N. R. Brown, S. Korolchuk, M. P. Martin, W. A. Stanley, R. Moukhametzianov, M. E. Noble, J. A. Endicott, *Nat. Commun.* **2015**, *6*, 6769.

SUPPORTING INFORMATION

Additional supporting information may be found online in the Supporting Information section at the end of the article.

How to cite this article: Kaur G, Cholia RP, Joshi G, et al. Anticancer activity of dihydropyrazolo[1,5-c]quinazolines against rat C6 glioma cells via inhibition of topoisomerase II. *Arch Pharm Chem Life Sci*. 2018;351:e1800023. https://doi.org/10.1002/ardp.201800023